

A recognition method of mineral shape based on extreme learning machine

In view of the situation of the existing algorithm for mineral shape recognition is relatively complex, the individual of strong pertinence and poor robustness, the use of infrared thermal images of minerals multifractal feature data classification recognition method is put forward. Multifractal can describe not only the local details, but also the overall characteristics that has the scale independence and theoretically is suitable for describing the texture characteristics and the distribution of mineral as well as that of energy resource. This paper uses multifractal as parameters of singularity detection of high-dimensional data and learning and understanding of high-dimensional data to distinguish the object/target from infrared heat map. The experimental result show that the infrared thermal image of mineral target in line with the multifractal characteristics, which can be used as one of the effective methods of infrared thermal images detection target. When three kinds of neural network ELM, PNN, GRNN is used for machine learning with obtain fractal parameters, ELM's accuracy is as high as 84%. While the same training with face natural images is done, ELM is still best, but accuracy is less than 15%. It shows that ELM combining with mineral fractal data has a better performance in classification and pattern recognition.

Keywords: Mineral recognition, mineral shape, feature data classification, extreme learning machine.

1. Introduction

Shape is one of the essential characteristics of the object. According to the principles of human vision, people rely mainly on contours and shapes to understand the image [1]. The shape feature is an important means to describe the high-level visual feature. To combine the underlying features of the image with the high-level features, there must be a good shape descriptor support. The

various shape descriptors were systematically summarized [2]. The principle of evaluating the merits of a shape descriptor is divided into a region-based approach, a contour-based approach, and a skeleton-based approach. The former uses the entire shape area of the information, all of which are derived from the target contour. He further divides the above method into structured and global methods according to the shape description. The structured method regards the shape as a combination of a series of shape primitives. The latter, skeleton, also known as the medial axis of the object [3], not only contains the geometrical features of the object shape, but also represents the object's topological structure.

There are many traditional contours based on contours. Kittler [4] classifies the shape of the contours. This classification is based on the new methods and new theories that have attracted wide attention in the last ten years. It is divided into four general methods, which are based on the method of spatial position relation of contour points, multi-scale method, transform domain method and new progress based on contour area. Based on contour shape representation method, this kind of method and the traditional shape descriptor based on area has a certain correlation. Based on the description of the area of traditional method made a great development in recent decades, including moment, Fourier descriptor, wavelet descriptor, morphological descriptions and good results have been obtained in the field of shape representation. The method based on region contains the shape of all pixels in the area of information, so that a class of descriptor is suitable for processing complicated shape, such as trademark, Chinese characters, etc. But the limitations of these methods is that they only contains the shape of the global information, the shape may be lost many important details.

The presentation of the mineral shape context representation can be considered as a milestone in the study of the mineral shape representation method. It is the most important method in the past decade. A large number of new methods and new theories are based on the representation of the mineral shape context. Compared to the traditional method, the disadvantage of these methods is that they only use the object boundary information and cannot reflect the mineral shape of the internal content of the object. The

Mr. Ding Dehong and Mss. Li Wuke, Li Hao and Li Ling, Hunan Province Cooperative Innovation Center for The Construction & Development of Dongting Lake Ecological Economic Zone, Hunan University of Arts and Science, Changde 415 000 and Mr. Ding Dehong, College of Electrical and Information Engineering, Hunan University, Changsha 410 082, China

advantage of multi-scale method is that they fully tap the mineral shape of the characteristics of a number of scales and step by step to reveal the mineral shape from the local details to the global overview of the information. The complexity of the multi-scale analysis is often higher and greatly increasing the workload and burden of processing on the scale of the work. Overall, the mineral shape of the overall characteristics and local characteristics of the effective combination of mineral shape to shape has become the main idea of the method based on the shape of the contour.

Mineral shape retrieval is the main application of mineral shape matching. John [5] proposed a method of co-transduction. The method is based on MPEG-7 CE-Shape-1 Part B, it makes the correct rate of retrieval improve to 97.72%, and it is the highest accuracy of the mineral shape retrieval method. Based on the local contour segment representation is an effective method in the classification of the mineral shape, a glimpse of the whole body in a pipe is the truth, how to define a significant part of the object, how to measure the different parts of the visual importance, how to describe the various parts of the scale and location relations, and these still remains in the stage of psychological exploration [6-7]. Machine learning and other intelligent algorithms will be more applied to the field of shape analysis, especially left a lot of research space in the matching space for structural excavation, and will have an important impact on areas such as natural image analysis. Based on the classification model of the neural network, the mineral body recognition was carried out based on the theory of the extreme learning machine (ELM).

2. Extreme learning machine

The classic form of SLFN is shown in Fig.1, which consists of the input layer, hidden layer and output layer. The input layer and the hidden layer, the hidden layer and the output layer are all connected in a full way. The output layer has m neurons corresponding to m output variables. The hidden

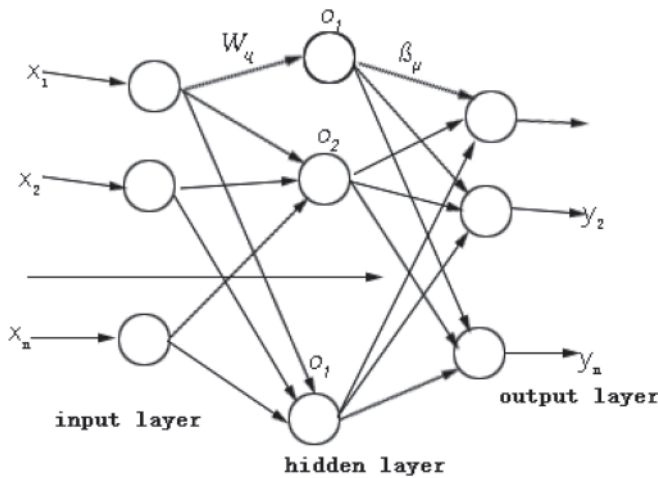


Fig.1 The structure of the typical single hidden layer feed forward neural network

layer has only one neuron. The input layer has n neurons corresponding to n input variables.

Suppose the connection weight between the input layer and the hidden layer is

$$w = \begin{bmatrix} \omega_{11} & \omega_{12} & \cdots & \omega_{1n} \\ \omega_{21} & \omega_{22} & \cdots & \omega_{2n} \\ \vdots & \vdots & & \vdots \\ \omega_{l1} & \omega_{l2} & \cdots & \omega_{ln} \end{bmatrix}_{l \times n} \quad \dots \quad (1)$$

where ω_{ji} represents the connection between the j neuron in the hidden layer and the i neuron in the input layer.

Suppose the connection β between the hidden layer and the output layer is

$$\beta = \begin{bmatrix} \beta_{11} & \beta_{12} & \cdots & \beta_{1m} \\ \beta_{21} & \beta_{22} & \cdots & \beta_{2m} \\ \vdots & \vdots & & \vdots \\ \beta_{l1} & \beta_{l2} & \cdots & \beta_{lm} \end{bmatrix}_{l \times m} \quad \dots \quad (2)$$

Among them, β_k represents the connection between the K neurons in the output layer and the j neurons in the hidden layer.

The threshold of the hidden layer neuron is

$$b = [b_1, b_2, \dots, b_l] \quad \dots \quad (3)$$

Then the training set (containing Q samples) of the input matrix and output matrix are

$$x = \begin{bmatrix} x_{11} & x_{12} & \cdots & x_{1m} \\ x_{21} & x_{22} & \cdots & x_{2m} \\ \vdots & \vdots & & \vdots \\ x_{n1} & x_{n2} & \cdots & x_{nm} \end{bmatrix}_{n \times Q}, \quad Y = \begin{bmatrix} y_{11} & y_{12} & \cdots & y_{1m} \\ y_{21} & y_{22} & \cdots & y_{2m} \\ \vdots & \vdots & & \vdots \\ y_{l1} & y_{l2} & \cdots & y_{lm} \end{bmatrix}_{m \times Q} \quad \dots \quad (4)$$

The activation function of the hidden layer neuron is $g(x)$, and the output of the network can be calculated by formula 1.

$$T = [t_1, t_2, \dots, t_Q]_{m \times Q}$$

$$t_j = \begin{bmatrix} t_{1j} \\ t_{2j} \\ \vdots \\ t_{mj} \end{bmatrix}_{m \times 1} = \begin{bmatrix} \sum_{i=1}^l \beta_{i1} g(\omega_i x_j + b_i) \\ \sum_{i=1}^l \beta_{i2} g(\omega_i x_j + b_i) \\ \vdots \\ \sum_{i=1}^l \beta_{im} g(\omega_i x_j + b_i) \end{bmatrix}_{m \times 1} \quad \dots \quad (5)$$

where $j = 1, 2, \dots, Q$, and $w_i = [\omega_{i1}, \omega_{i2}, \dots, \omega_{in}]$,

$$x_j = [x_{1j}, x_{2j}, \dots, x_{nj}]^T.$$

Type (5) can be expressed as

$$H\beta = T \quad \dots \quad (6)$$

Among them, H is the output matrix of hidden layer.

$$H(w_1, w_2, \dots, w_1, b_1, b_2, \dots, b_1, x_1, x_1, \dots, x_Q) = \begin{bmatrix} g(w_1x_1 + b_1) & g(w_2x_1 + b_1) & g(w_1x_1 + b_1) \\ g(w_1x_2 + b_1) & g(w_2x_2 + b_1) & g(w_1x_1 + b_1) \\ \vdots & \vdots & \vdots \\ g(w_1x_Q + b_1) & g(w_2x_Q + b_1) & g(w_1x_Q + b_1) \end{bmatrix}_{Q \times 1} \quad \dots \quad (7)$$

Based on previous research results, Huang et al summed up the following two conclusions [8-9].

Conclusion 1: Given sample (x_i, t_i) ,

$$x_i = [x_{i1}, x_{i2}, \dots, x_{in}]^T \in R^n, t_i = [t_{i1}, t_{i2}, \dots, t_{in}] \in R^m,$$

and activation function: $R \rightarrow R^n$, then, for SLFN with Q - hidden layer, the hidden layer output matrix H is invertible and $\|H\beta - T\| = 0$ in the case of any assignment $b \in R$ and $w_i \in R^n$.

Conclusion 2: Given sample (x_i, t_i) ,

$$x_i = [x_{i1}, x_{i2}, \dots, x_{in}]^T \in R^n, t_i = [t_{i1}, t_{i2}, \dots, t_{in}] \in R^m$$

and activation function $g: R \rightarrow R^n$, any small positive error ε , then, there is always a SLFN, whose hidden layer contains the number of neurons not exceeding the number of samples, and in the case of any assignment $b \in R$ and $w_i \in R^n$, there is $\|H_{N \times M} \beta_{N \times M} - T\| < \varepsilon$.

From the above two conclusions can be drawn: when the activation function $g(x)$ is infinitely differentiable in any interval, the W and B can be determined by random selection before training, and do not have to change in the training process, also don't have to adjust all parameters of SLFN. By solving the solution of (8), the connection β between the hidden layer and the output layer can be obtained.

$$\min_{\beta} \|H\beta - T\| \quad \dots \quad (8)$$

Solvable

$$\hat{\beta} = H^+ T' \quad \dots \quad (9)$$

H^+ is the generalized inverse of Moore-Penrose for H .

3. Mineral shape recognition based on extreme learning

In many areas, SLFN has been recognized by academics with excellent learning performance [10]. However, the traditional neural network learning algorithm is also inadequate. Because the gradient is usually used algorithm, feed forward neural network is showing the following points.

(1) It is difficult to achieve the global optimal, and it is easy to fall into the local extreme.

(2) Training is slow.

(3) The value of the learning rate is very sensitive, it is not easy to choose the best.

Therefore, it is always the goal of the researchers to find the algorithm which is easy to control, has good generalization ability, fast and can obtain the global optimal solution, and is used to improve the performance of RBF. This section introduces the extreme learning machine (ELM) algorithm, which is dedicated to SLFN and improves its performance. The algorithm first sets the number of neurons in the hidden layer, without the need to preset other parameters. The thresholds and connection weights of the neurons are randomly generated during the training process, and no adjustment is needed. After the training, the global optimal solution can be obtained. Simulation results show that the algorithm has good generalization ability, simple operation, fast speed and so on. Finally, this section uses multiple extracted features, and uses this algorithm, BP, GRNN, PNN and RBF to compare and evaluate their advantages and disadvantages.

3.1 PROCESS OF ELM LEARNING ALGORITHM

The process of ELM learning algorithm based on the conclusion of the previous section is summarized in Fig.2.

According to the above related algorithms and conclusions, two ELM functions are developed in Matlab environment.

Training function is ELM train, [IW, B, LW, TF, TYPE] = ELM train (P, T, N, TF, TYPE).

Predictive function is ELM predict Y = ELM predict (P, IW, B, LW, TF, TYPE).

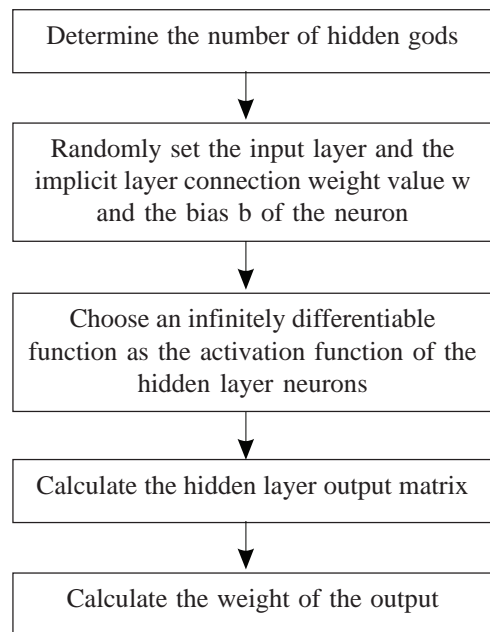


Fig.2 The process of ELM learning algorithm

TABLE 1: INPUT MODEL OF FOUR VARIABLES

Model number	1	2	3	4	5	6	7	8	9	10
Enter the attribute										
Maximum a	■	■	■	■						
Minimal a		■	■	■	■	■	■			
Difference a			■	■		■	■	■	■	
Frequency difference				■			■		■	■

Among them, ■ indicates the establishment of the corresponding input attribute participation model

Among them, IW is the connection weight between the input layer and the hidden layer. B is the threshold of hidden layer neurons. LW is the connection weight between the hidden layer and the output layer. TF is the activation function of hidden layer neurons, whose value is 'sig' (default), 'sin', 'hardlim'. $TYPE$ is an application type of ELM with a value of 1 (default, indicating classification) and 0

(regression and fit). P is the input matrix of the training set. T is the output matrix of the training set. N is the number of neurons in the hidden layer (the number of samples that default to the training set). The output of the training function is the input of the predictive function, and the Y is the output prediction corresponding to the test set.

3.2 ELM WILDLIFE CLASSIFICATION MODELING

In order to evaluate the performance of ELM, ELM was applied to the classification of mammals, and the results were compared to the performance and operation speed of traditional feed forward networks (BF, RBF, GRNN, PNN) and discusses the contrast effect after using PCA dimension reduction.

According to the requirements of the problem description, to achieve ELM algorithm machine learning, roughly divided into the following steps: data set (training set and test set), training, simulation test, as shown in Fig.3.

There are 7 input variables, and in the case of no prior gravity, the contribution of variables to classification is not known. Therefore, the full combination of variables is used as input model, and when there are 7 variables, there are 28 input models. After doing the PCA (principal component analysis) of the 7 variables, they can be reduced to 4 variables. Taking 4 variables as an example, there are 10 input models as shown in Table 1.



Fig.3 ELM model framework

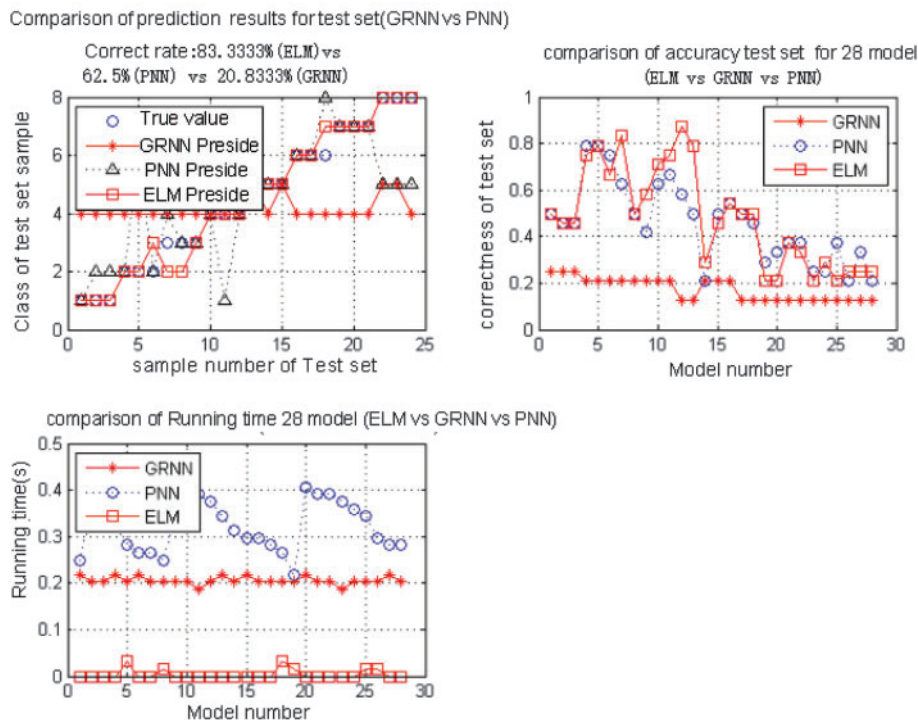


Fig.4 The original data and effect of mineral infrared

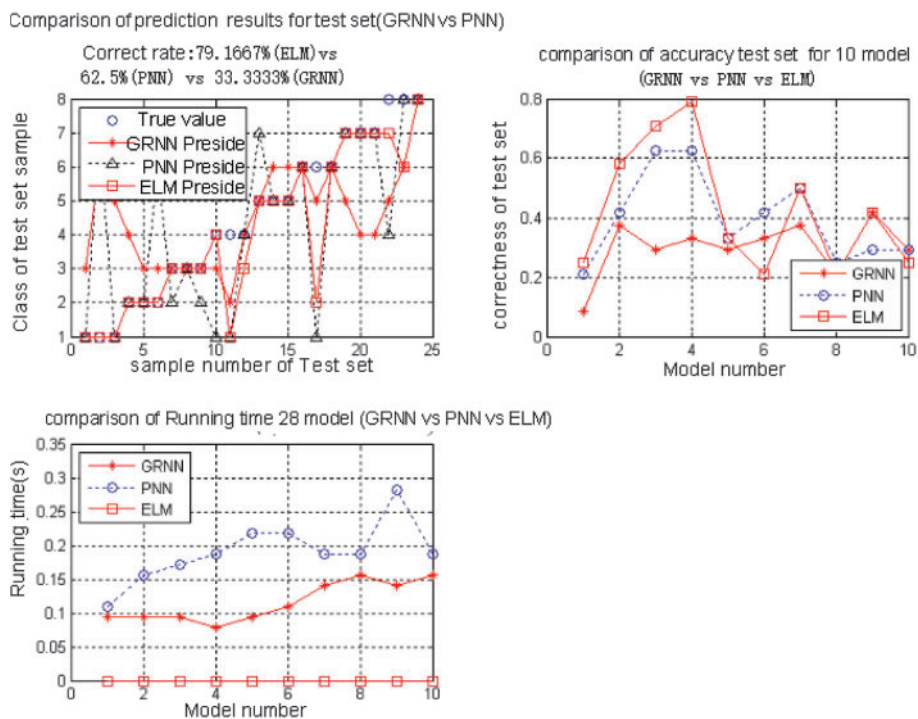


Fig.5 PGA data and effect of mineral infrared

4. ELM recognition results

From the analysis of Fig.4, it can be concluded that the prediction accuracy of ELM, PNN, and GRNN were: 84%, 62.5% and 33.3% respectively using raw fractal data. The

prediction accuracy of ELM, PNN, and GRNN after fractal data PCA was: 79%, 62.5% and 33.3% respectively. This shows that ELM has good performance in classification and pattern recognition of animal fractal data.

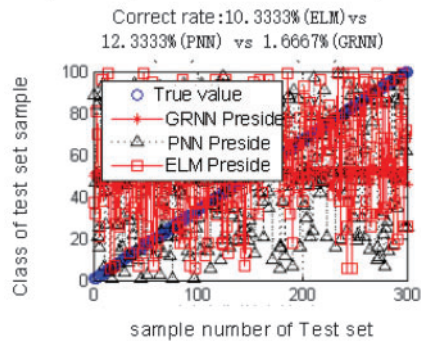
From the analysis of Fig.5, it can be concluded that when 120 samples are used for pattern recognition, the run time averages of PNN, GRNN and ELM are 0.2s, 0.1s, 0.01s (running configuration is different, the result will be different, the same), which indicates that the ELM has an absolute advantage over GRNN on the computational speed, and GRNN is about twice as good as PNN.

From the analysis of Fig.6, it can be concluded that when the programme classifies 120 samples with three algorithms, the running time is 6.678s and 3.119 seconds and the image processed per second > 24 meet the requirements of real-time dynamic processing in the case of data without PCA and PCA. After PCA is performed on the data, it can obviously improve the operation speed and slightly more than 1 times.

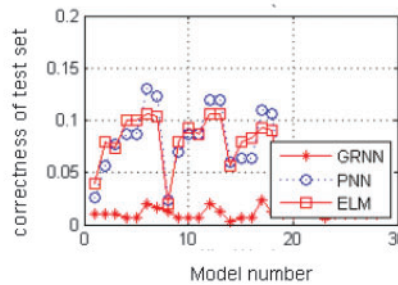
5. Conclusion

With multiple mineral shape features of infrared image from Figs.4-6 the effect of mineral target, ELM is an effective method to detect the mineral target infrared image. After obtaining the fractal data, the ELM, PNN and GRNN neural networks are used to study the machine. It is found that the correct rate of ELM is as high as 84%, while the same training is done with the natural image of the mineral, although the ELM is still the best, rate of less than 15%. This shows that ELM is the best performance in the use of mineral fractal data classification and pattern recognition applications. From another point of view, it is assumed that the fractal features of the natural light image of the mineral are not obvious, and this hypothesis

Comparison of prediction results for test set (GRNN vs PNN)



comparison of accuracy test set for 28 model (ELM vs GRNN vs PNN)



comparison of Running time 28 model (ELM vs GRNN vs PNN)

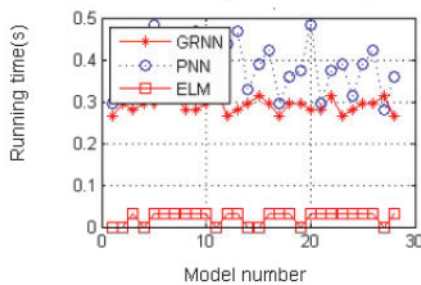


Fig.6 The data of visible light and effect of classification

needs further proof. If the multifractal feature can combine the mineral shape and direction of the region, the recognition rate can be further improved. The above research has some reference and reference for oil and gas target delineation.

Acknowledgements

This work is supported by Hunan province key high-tech project (Grant No. 2016GK2019). The general project of Hunan province department of education (Grant No. 16C1089), and Dr. Launch funds of the scientific research of Hunan University of Arts and science.

References

- Xu, L., Krzyzak, A. and Suen, C. (1992): "Methods of Combining Multiple Classifiers and Their Applications to Handwriting Recognition." *IEEE Transactions on Systems, Man and Cybernetics*. 1992, 22(3): 418-435.
- Brunelli, R. and Falavigna, D. (1995): "Person Identification Using Multiple Cues." *IEEE Transactions on PAMI*. 1995, 12: 955-966.
- Hong, L. and Jain, Anil K. (1998): "Integrating Faces and Fingerprints for Personal Identification." *IEEE Transactions on PAMI*. 1998, 20: 1295-1307.
- Kittler, J., Hatef, M., Duin, R. P. and Matas, J. G. (1998): "On Combining Classifiers." *IEEE Transactions on PAMI*. 1998, 20: 226-239.
- Daugman, John G. (1993): "High Confidence Visual Recognition of Persons by a Test of Statistical Independence." *IEEE Transactions on PAMI*. 1993, 15(11):1148-1161.
- Ross, Arun and Jain, Anil K. (2003): "Information Fusion in Biometrics." *Pattern Recognition Letters*. 2003, 24: 2115-2125.
- Ross, A., Jain, Anil K. and Reisman, J. (2003): "A Hybrid Fingerprint Matcher." *Pattern Recognition*. 2003, 36: 1661-1673.
- Mandelbrot, B. B. and Evertsz, C. J. G. (1990): "The potential distribution around growing fractal clusters." *Nature*, 1990, 348(6297):143.
- Jian, Yang (2003): "Feature fusion: parallel strategy vs. serial strategy." *Pattern Recognition*. 2003, 36(6): 1369-1381.
- Cao, Jiawu and Zhu, Qiuyu (2002): "A Contour-based Image Retrieval Algorithm." *Computer Engineering*, 2002, 28(7):159-160.

RESEARCH ON CHANGE OF MICRO-STRUCTURE AND MECHANICAL PERFORMANCE Si/C MATRIX COMPOSITES FOR THERMAL PROCESS

(Continued from page 861)

- Bouillon, E., Langlais, F. and Pailler, R., et al. (1991): *Journal of Object Science*, 1991, 26 (5): 1333-1345.
- Biernacki, J. and Wotzak, G. (1989): *Journal of the American Ceramic Society*, 1989, 72 (1): 122.
- Koumoto, K., Takeda, S. and Pai, C., et al. (1989): *Journal of the American Ceramic Society*, 1989, 72 (10): 1985-1987.
- Ferrari, A. and Robertson, J. (2000): *Physi/Cal Review B*, 2000, 61: 14095-14107.
- Tuinstra, F. and Koenig, J. (1970): *The Journal of Chemical Physi/Cs*, 1970, 53: 1126-1130.
- Yu, X., Zhou, W. and Zheng, W., et al. (2009): *Rare Metal Object and Engineering*, 2009, 38(z2): 462-465.
- Zhou, X., You, Y. and Yu, H., et al. (2008): *Rare Metal Object and Engineering*, 2008, 37 (z1): 32-35.
- Li, J., Zhang, L. and Cheng, L., et al. (2007): *Rare Metal Object and Engineering*, 2007, 36 (9): 1539-1544.
- Soraru, G., Babonneau, F. and Mackenzie, J. (1990): *Journal of Object Science*, 1990, 25: 3886-3893.
- Despres, J. F. and Monthieux, M. (2009): *J. Eur. Ceram. Soc.*, 2009(2): 30-33.
- Yan, Zheyu, Xu, Qiang and Zhu, Shizhen, et al. (2011): *Rare Metal Material And Engineering*, 2011, 40(z1): 623-626.
- Bunsell, A. R. and Piant, A. (2006): *Journal of Materials Science*, 2006, 41(3): 823-839.